J Mol Model (2005) 11: 370–378
DOI 10.1007/s00894-005-0261-x

ORIGINAL PAPER

Bartłomiej Szyja · Jerzy Szczygieł · Iwona Tymków

Effect of Pt and Sn on the adsorption of *n*-heptane in γ-Al_2O_3 catalyst models

Received: 2 November 2004 / Accepted: 17 February 2005 / Published online: 12 May 2005

Abstract The Grand Canonical Monte-Carlo (GCMC) method has been used to carry out simulations of the adsorption of *n*-heptane in models of naphtha-reforming catalysts. Models used in the study differed in the number and distribution of metal atoms—Pt and Sn. The number of adsorbed *n*-heptane molecules grows linearly with increasing number of metal atoms. The effect of Pt content on the adsorption of *n*-heptane molecules is most distinct at approximately 100 kPa and within the lower range of the temperatures investigated. In the models of bimetallic catalysts, the effect of the two metals is additive.

Keywords Sorption · γ-Al_2O_3 · Reforming · Hydrocarbons · GCMC

Introduction

The majority of chemical processes occur in the presence of catalysts. The mechanisms governing the performance of many catalysts are still far from being well understood. Knowledge of energetically beneficial locations, interaction energy and the potential for diffusion of organic molecules in microporous solid structures is a prerequisite for the appropriate understanding of adsorptive and catalytic behavior. The past decade has witnessed the development of many sophisticated computer-based calculationed methods that offer the possibility of acquiring such knowledge. With the information acquired by using these methods, it is possible not only to interpret the experimental results but also to gain insight into the properties of the catalytic system, some of which would have never been disclosed if we had contented ourselves with experiments alone. Since the properties of catalytic systems (activity and selectivity) depend strongly on the interactions between the host and the guest atoms, it is necessary to analyze the phenomena occurring in the catalyst interior at the molecular level.

Implemented on an industrial scale in 1949 and conducted over bifunctional, Pt-containing catalysts, the reforming process yields high-octane petrol enriched with aromatic hydrocarbons [1]. Continuing technological advance has raised the demands made on the reforming catalyst, which must display high selectivity (enabling performance at elevated temperatures without a noticeable rise in the rate of the hydrocracking reaction), high coking resistance, and high immunity to frequent regeneration.

Catalysts with such properties, e.g. bimetallic Pt–Re/γ-Al_2O_3, have been in use since the 1960 s [2]. They are able to perform at elevated temperatures, pressures approaching 20 atm. and an H:HC ratio below 8:1. Presently, platinum is often combined with tin [3], which leads to a slight decrease in catalytic activity and a rise in the stability of the system. However, the incorporation of tin into the catalyst has disadvantages. According to Burch and Garla [4, 5], the presence of tin modifies both the acidity of Al_2O_3 and the electron structure of Pt. Arteaga et al. [6] have found that tin noticeably affects the selectivity of the catalyst.

The structure of the active centers (platinum) depends to a large extent on the preparation method. The presence of chlorine favors the formation of Pt^0–Sn^0 alloys [7] or the incorporation of Sn (in oxide form) into the support structure [7,8,9].

Aim and scope of the study

The paper describes an application in which molecular modeling methods apply, enabling a better understanding, a more reliable interpretation and, to a certain degree, the prediction of the behavior of the catalytic system. The objective of the study reported in this paper

---

B. Szyja (✉) · J. Szczygieł · I. Tymków
Institute of Chemistry and Technology of Petroleum and Coal,
ul. Gdańska 7/9, 50-344 Wrocław, Poland
E-mail: sbart@pwr.wroc.pl

was to model the adsorption and diffusion of *n*-heptane in the following reforming catalysts: Pt/γ-Al_2O_3, Sn/γ-Al_2O_3 and Pt–Sn/γ-Al_2O_3, in order to determine the effect of the two active metals on both physicochemical phenomena, which are the key stages of catalytic chemical reactions.

Model and computational details

Nine modified models were used to simulate the adsorption of *n*-heptane on the support and on the aluminum oxide (γ-Al_2O_3) reforming catalyst. The models were constructed based on the cell parameters and atom coordinates coming from the Cerius^2 model library [10].

The size of the model was increased to four elementary cells in the directions of the *x*-axis and *y*-axis, as well as seven cells in the direction of the *z*-axis. Next, some of the atoms were removed in order to form a 16 Å diameter micropore in the crystalline structure along the longest side of the system. The shape and the size of the micropore were chosen arbitrarily. The porous structure of the γ-Al_2O_3 catalyst is highly irregular, with a pore size varying from several Å (micropores developing on the catalyst surface) to several thousand Å (macropores responsible for the transport of reagents). Adsorption of reforming reagents occurs in micropores of diameters ranging between several and several dozen Å, so we decided to use this pore size in our models.

In this way, a supercell consisting of 112 cells was obtained and periodical boundary conditions were applied. Thus, we assumed that the model is built of an infinite number of micropores arranged in parallel, which do not intersect at any point (Fig. 1).

In this way, we constructed the initial model of the support, which served for preparation of the final catalyst models made use of in the simulations. The support model consisted approximately of 10,000 at. To determine the energy for such a large systems, it is advisable to use the force-field method, which yields reliable results at a comparatively low computational cost.

The force field gives an expression describing the potential energy surface for a given model as a function of atomic coordinates. The total potential energy of the system (E_{total}) is expressed as the sum of the energy resulting from the chemical bond length (E_{bond}), the energies of angle bending (E_{angle}) and dihedral angle bending ($E_{dihedral}$) between atoms, and the energy of the cross-terms describing the interactions between lengths and angles ($E_{cross\text{-}term}$). If the system consists of more than one molecule, a term describing the energy of nonbonding van der Waals (E_{vdW}) and Coulomb ($E_{Coulomb}$) interactions is introduced. Then we have

$$E_{total} = E_{bond} + E_{angle} + E_{dihedral} + E_{\text{cross - term}} + E_{vdW} + E_{Coulomb}$$

To analyze the adsorption phenomenon, we made use of the Grand Canonical Monte-Carlo (GCMC) ensemble [11, 12]. In the course of the simulation process, the chemical potential (μ), the volume of the system (V) and

Fig. 1 Support model

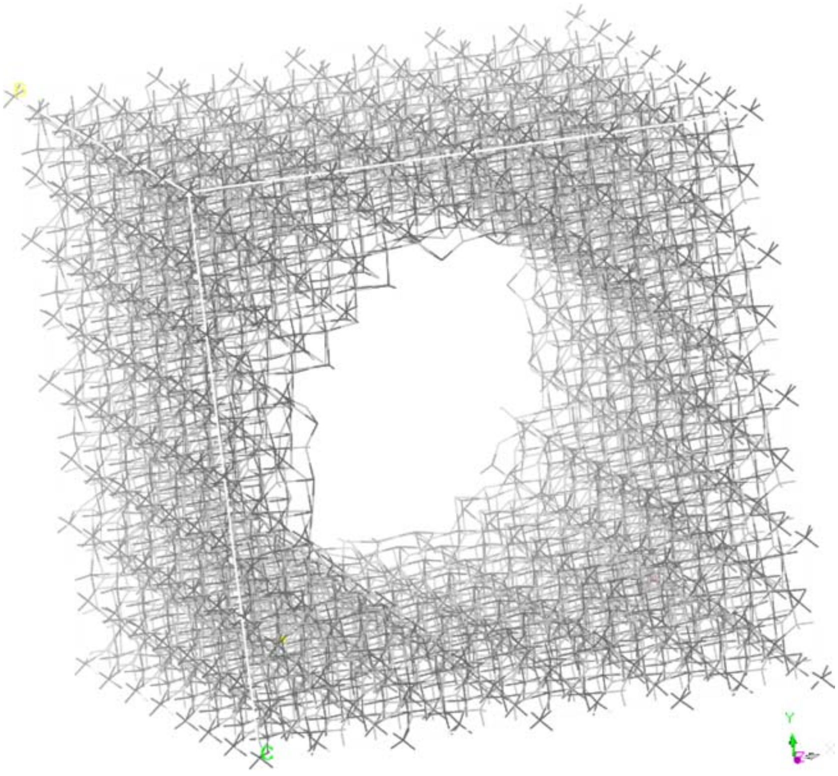

temperature (*T*) were constant. The method involves multiple sampling of the guest molecule position, as well as the creation of new molecules and destruction of existing molecules in the micropores of the host. The state obtained in this way is accepted with a probability depending on the system energy. The procedure is repeated enough times to be statistically significant and enable thermodynamic equilibrium to be achieved (Scheme 1).

Considering the readiness of *n*-heptane to produce a variety of conformers, we established a library comprising ten of these prior to the main simulation procedure. Sampling was repeated for each of the systems of hydrocarbon atoms generated.

Making use of the support model already constructed, we built five Pt/γ-Al_2O_3 catalyst models where a certain part of the Al atoms on the micropore surface was replaced with Pt atoms, their number ranging from 1 in model 1 to 9 in model 5. Thus, each further model contained two more atoms than the previous model. The Pt content ranged between 0.21 and 1.84 wt.%. A similar method was used to construct the Sn/γ-Al_2O_3 catalyst models, where the Sn content varied from 0.13 wt.% (1 at./cell) to 1.13 wt.% (9 at./cell). Our simulations also involved 25 Pt–Sn/γ-Al_2O_3 catalyst models containing one three, five, seven or nine Pt and Sn atoms. In each case, the places for the atom substitution were chosen randomly.

Energy minimization was carried out by the Universal force-field method [13–15] with all the models, thus enabling the most stable configuration of the system to be found. The choice of this force field is substantiated by the observation of the unit cell geometry, as shown in Fig. 2. The GCMC simulations were repeated at pressures varying from 0.01 to 100,000 kPa and temperatures ranging between 573 and 973 K. Use was made of CVFF [16–24] since with this force field our tentative simulations yielded more consistent results than those obtained with the UFF. We did not modify the force fields for the need of our study either in the range of atom parameters or in the functional form.

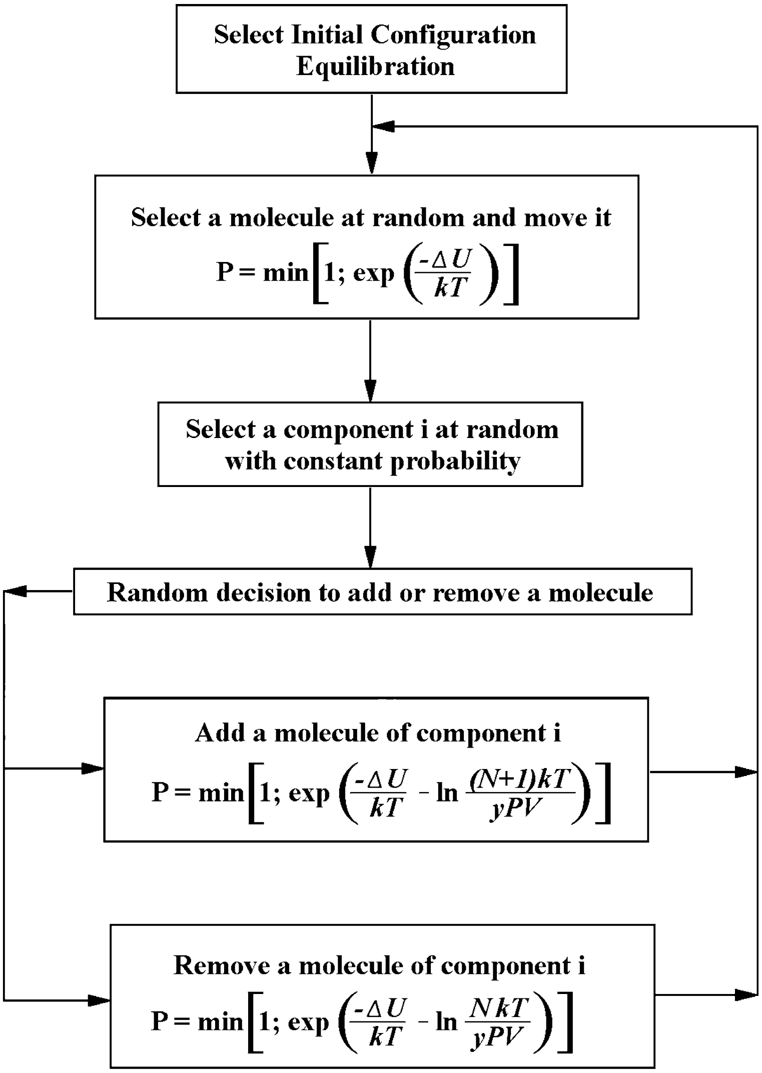

Scheme 1 The Grand Canonical Monte-Carlo (GCMC) methodology

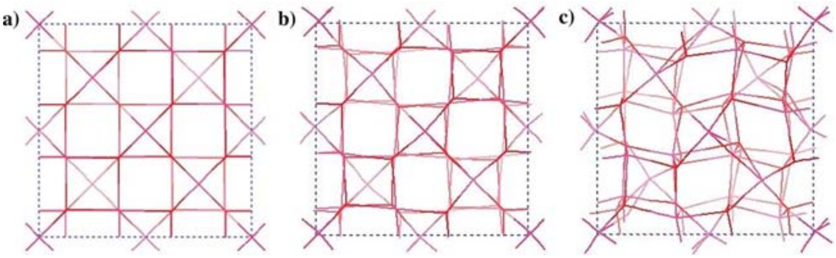

Fig. 2 Crystallographic data of γ-Al_2O_3 (a) compared to the same structure optimized with UFF (b) and CVFF (c)

The number of steps, which was chosen according to the pressure applied, varied from 1 million at 0.01 kPa to 12.5 million at 100,000 kPa. To be sure that the system had achieved the equilibrium state, we carefully observed such parameters of simulation as creation/destruction ratio and the ratio of accepted to total tries of molecular translation or rotation. Due to the small number of *n*-heptane molecules present in the micropores in low pressure, the system achieved the equilibrium state in a very short time, and chosen number of steps was more then enough.

Results

Unlike the computer-simulated results for zeolites, those for the reforming catalyst model are difficult to verify via experiment because of the disordered structure of the aluminum oxide used as catalyst support. This disorder is to be attributed to lattice defects, as well as to the presence of a great number of micropores and macropores differing in shape and size. It should also be noted that the Pt/γ-Al_2O_3 system is a very reactive one. Under real conditions it is impossible to observe the adsorption of a single hydrocarbon on the catalyst surface because an equilibrium between the substrates and the reaction products will soon be established.

Pt/γ-Al_2O_3 catalyst

The results obtained are presented as the adsorption isotherms for a determined temperature and a defined number of atoms of the active metals included in the models. Figure 3 shows that a rise in temperature generally decreases the extent of adsorption. This result may seem to be trivial, but the qualitative agreement between the results and real observations of the temperature effect on adsorption substantiates the reliability of the model adopted for the computations. The number of molecules adsorbed at 773 K is very small even at a pressure of 100 kPa. A further rise in pressure increases the number of the *n*-heptane molecules adsorbed, but this number is lower than the one at 473 K and the same pressure. At 473 K it is clearly seen that the amount of *n*-heptane adsorbed increases at high pressure, but this increase is very small since the active centers become saturated with the adsorbed substance. Such phenomena did not occur with the other temperatures investigated.

To analyze the effect of the amount of Pt in more detail, some sections of the isotherms at 773 K and pressure approaching 1000 kPa were plotted. The isotherms in Fig. 4 are ascending lines, and their gradient increases with increasing number of Pt atoms.

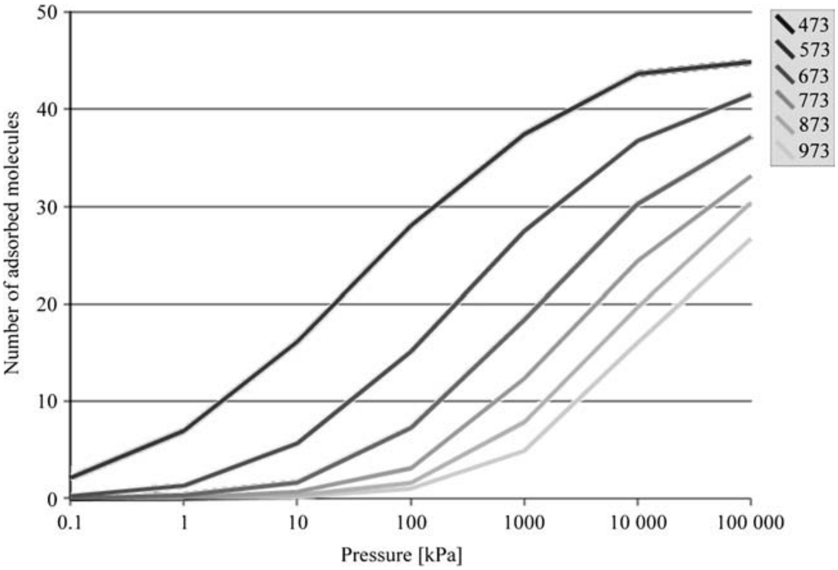

Fig. 3 Isotherms of adsorption of n-heptane on Pt/γ-Al_2O_3 catalyst (9 at./cell) under conditions of simulations

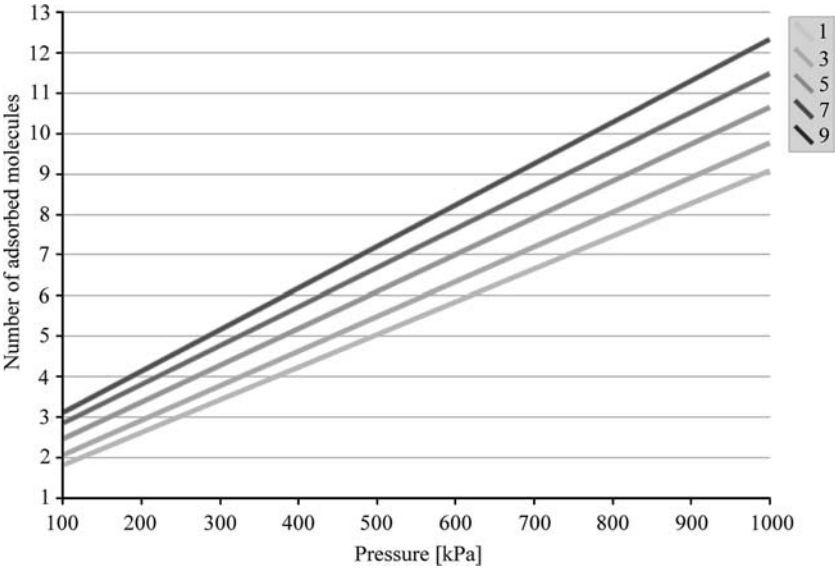

Fig. 4 Fragments of isotherms of adsorption of n-heptane on models of Pt/γ-Al_2O_3 catalyst containing one, three, five, seven and nine Pt atoms in supercell (773 K and 100–1000 kPa)

The increase in Pt content is paralleled by a slight increase (compared to that in temperature or pressure) in the number of adsorbed *n*-heptane molecules. This increase is of a linear nature (Fig. 5). The slopes of the straight lines approximating the relation between the number of adsorbed *n*-heptane molecules and the number of Pt atoms in the catalyst model for various temperatures and pressures are shown in the form of scattered points in Fig. 6.

As shown in Fig. 6, the effect of Pt content on the adsorption of *n*-heptane molecules is most distinct at approximately 100 kPa and within the lower range of temperatures investigated, and the poorest within the higher temperature range and at lower pressure. The characteristic "ridge" in Fig. 6 indicates that in the entire temperature range investigated (473–1073 K) the effect of Pt on the extent of adsorption is particularly pronounced at pressures ranging between 100 and 1000 kPa.

Approximation of the slope values with a quadratic polynomial is of a qualitative rather than quantitative nature because of a comparatively low correlation coefficient (0.710). It may, however, be expected that the favorable effect of Pt, which facilitates adsorption, will increase further with dropping temperature.

Sn/γ-Al_2O_3 catalyst

The effect of Sn on the γ-Al_2O_3 catalyst is similar to that of Pt. The number of guest molecules adsorbed increases with increasing number of Sn atoms. Again, this can be attributed to the higher number of available active centers, which means that there was a greater amount of potential sites for the hydrocarbon molecules to bind to. A rise in temperature was paralleled by a decrease in the amount of the molecules adsorbed. Thus, over a catalyst

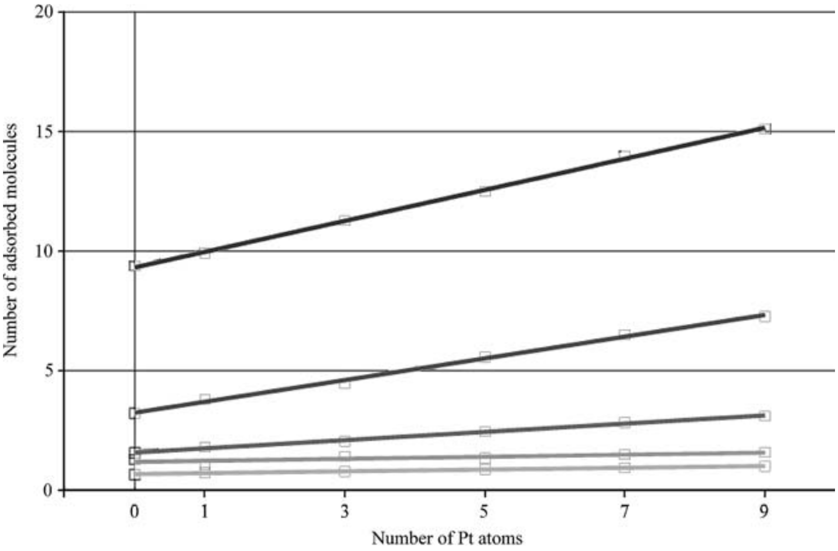

Fig. 5 Number of adsorbed guest molecules related to the number of Pt atoms at 573–973 K and 100 kPa. Linear approximation

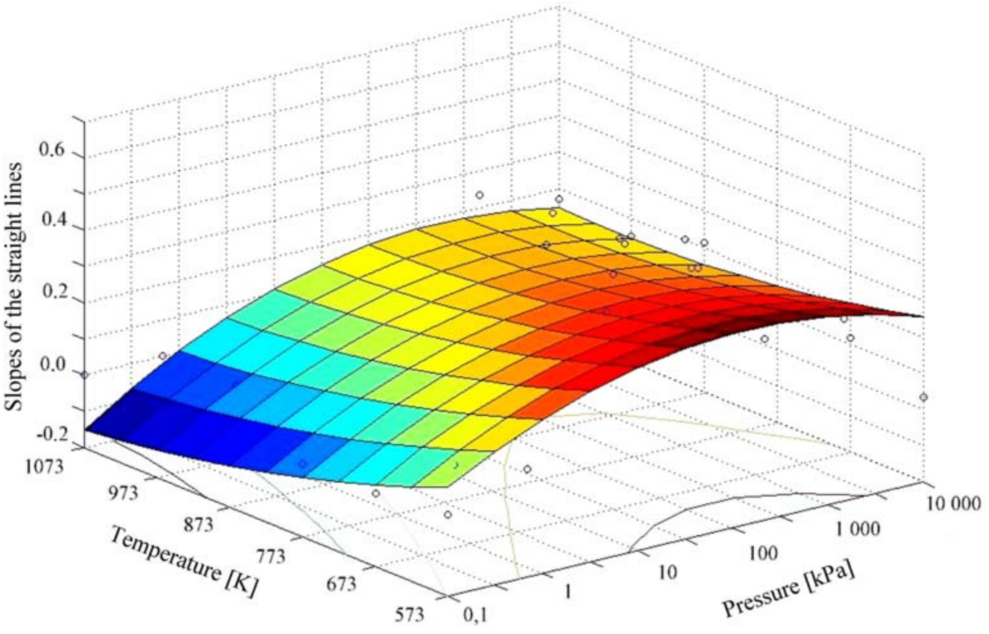

Fig. 6 Pressure and temperature dependent slopes of the straight lines approximating the relationship between the amount of molecules adsorbed and the amount of platinum

doped with one Sn atom, at a pressure of 100,000 kPa, the number of guest molecules adsorbed dropped from 39 to 21.5 at 573 and 1073 K, respectively. (It is worth noting that over a catalyst with a single Pt atom, under equivalent temperature and pressure conditions, almost the same values were obtained: 38.4 and 21.2.) A rise in pressure also accounted for a remarkable increase in the number of the molecules adsorbed.

All of the isotherms have a feature in common. At 1000 kPa and higher pressure, the lines relating the extent of adsorption to the pressure applied are closer to each other for the catalysts with one and three Sn atoms and remarkably farther from the isotherms for the catalysts with five, seven and nine Sn atoms (Fig. 7). Such behavior does not seem to be accidental. In order to explain this pattern, we analyzed the structure of the model and the arrangement of the Sn atoms on the support. When constructing the model, we assumed a random, automatically generated distribution of the metal atoms on the support surface. Thus, the model contained two Sn atoms situated at a short distance from each other (12.4 Å). As a result, the *n*-heptane molecule adsorbed at one of the Sn centers may inhibit the access to the other Sn center. The distance, however, was far enough to prevent a single molecule from blocking both centers; though adsorption in one of them may become difficult (Fig. 8).

Using the linear approximation (slopes of the straight lines) of the relationship between the number of the guest molecules adsorbed and the number of Sn atoms incorporated in the host model for various temperatures and pressures, we obtained 3D plots (Fig. 9) that reflect the influence of the Sn amount on the adsorption of *n*-heptane on the Sn/γ-Al_2O_3 catalyst. (The slopes of the straight lines are shown in the form of scattered points.) This influence becomes visible in the range of higher

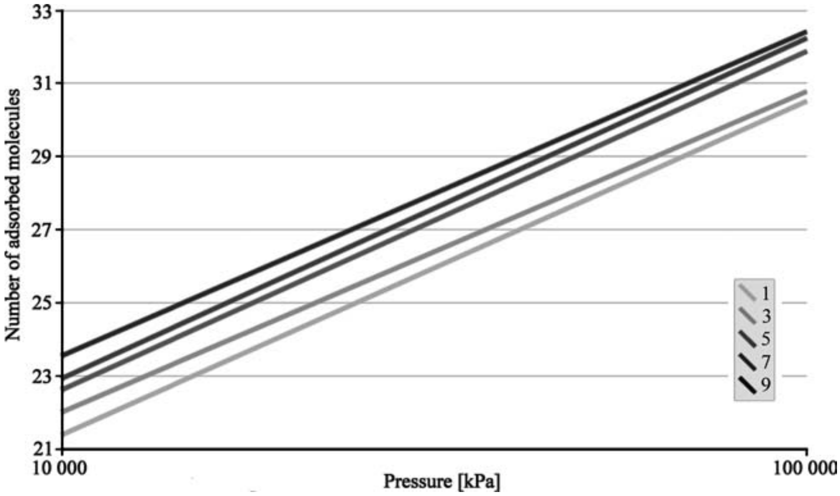

Fig. 7 Fragments of isotherms of adsorption of n-heptane on Sn/γ-Al_2O_3 catalyst containing one, three, five, seven and nine Sn atoms in supercell (773 K and 10,000–100,000 kPa)

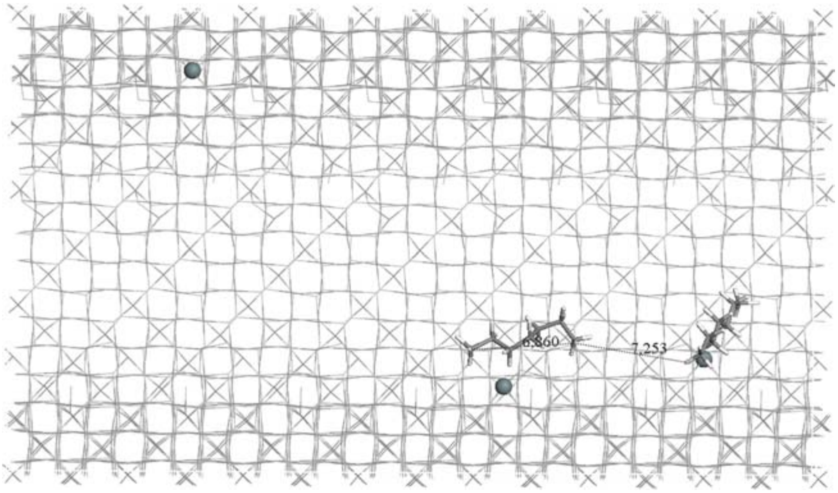

Fig. 8 Distance between Sn atoms in the Sn(3)/γ-Al_2O_3 catalyst (cross-section of the catalyst)

pressures, but is smaller than that of the amount of Pt in the Pt/γ-Al_2O_3 catalyst. The effect of Sn on the extent of adsorption in the investigated pressure and temperature range is the strongest at 573 K and 10,000 kPa and becomes weaker towards higher temperature and lower pressure. A similar pattern was observed in the Pt/γ-Al_2O_3 catalyst model (Figs. 6, 9).

Again, because of the relatively low correlation coefficient (0.64), the approximation of the slope values with a quadratic polynomial is of a qualitative rather than quantitative nature.

Pt–Sn/γ-Al_2O_3 catalyst

The isotherms of adsorption for the catalysts investigated, Pt/γ-Al_2O_3, Sn/γ-Al_2O_3 and Pt–Sn/γ-Al_2O_3, are compared in Fig. 10. The lines are identical in shape regardless of the pressure applied. Thus, the catalysts of an increasing adsorptive capability can be arranged in the following order:

$$\mathrm{Pt-Sn}/\gamma\text{ - }\mathrm{Al_2O_3} > \mathrm{Pt}/\gamma\text{ - }\mathrm{Al_2O_3} > \mathrm{Sn}/\gamma\text{ - }\mathrm{Al_2O_3}$$

Additionally, comparing the number of Pt and Sn atoms, we obtain:

$$\begin{aligned}&\mathrm{Pt-Sn}/\gamma-\mathrm{Al_2O_3}(\mathrm{Pt}\ 7,\ \mathrm{Sn}\ 7) >\\ &\mathrm{Pt-Sn}/\gamma-\mathrm{Al_2O_3}(\mathrm{Pt}\ 7,\ \mathrm{Sn}\ 1) > \mathrm{Pt}/\gamma-\mathrm{Al_2O_3}(\mathrm{Pt}\ 7)\\ &\gg \mathrm{Pt-Sn}/\gamma\text{ - }\mathrm{Al_2O_3}(\mathrm{Pt}\ 1,\ \mathrm{Sn}\ 7) > \mathrm{Sn}/\gamma\text{ - }\mathrm{Al_2O_3}(\mathrm{Sn}\ 7)\end{aligned}$$

Since the Pt–Sn/γ-Al_2O_3 (Pt 7, Sn 7) catalyst displays twice as many active centers as the other catalysts, it is not surprising that the greatest number of *n*-heptane molecules is adsorbed there. The order substantiates the greater potential of adsorption for Pt than for Sn, as seen in the amounts of molecules adsorbed.

Figure 11 shows the joint influence of Pt and Sn on the number of *n*-heptane molecules adsorbed at 773 K at an increasing pressure. As shown by these 3D plots, the number of adsorbed molecules increases with increasing pressure. For each pressure value applied, the number of the *n*-heptane molecules adsorbed rises as the number of

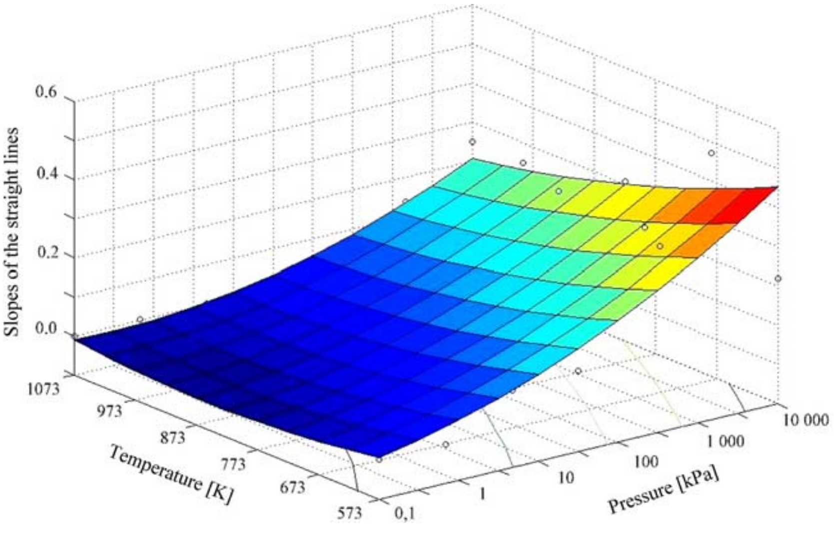

Fig. 9 Pressure and temperature dependent slopes of the straight lines approximating the relationship between the amount of molecules adsorbed and the amount of tin

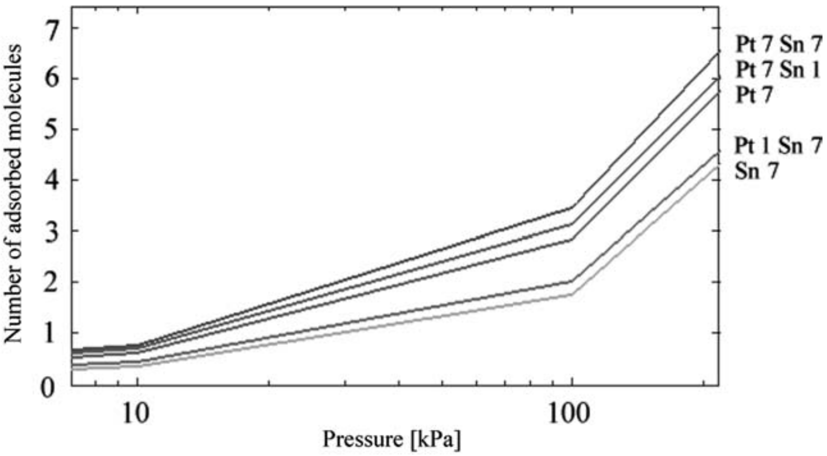

Fig. 10 Comparison of adsorption isotherms for Pt/γ-Al_2O_3, Sn/γ-Al_2O_3 and Pt–Sn/γ-Al_2O_3 catalysts at 773 K

Pt and Sn atoms increases. This rise however, is much greater with the increase in the number of Pt than Sn atoms. For example, at 773 K and 10 kPa, the number of adsorbed molecules for one Pt atom and one Sn atom amounts to 0.433; for one Pt atom and nine Sn atoms only 0.462; for nine Pt atoms and one Sn atom as much as 0.803, and for nine Pt atoms and nine Sn atoms 0.870. The same pattern was observed at other temperature and pressure conditions.

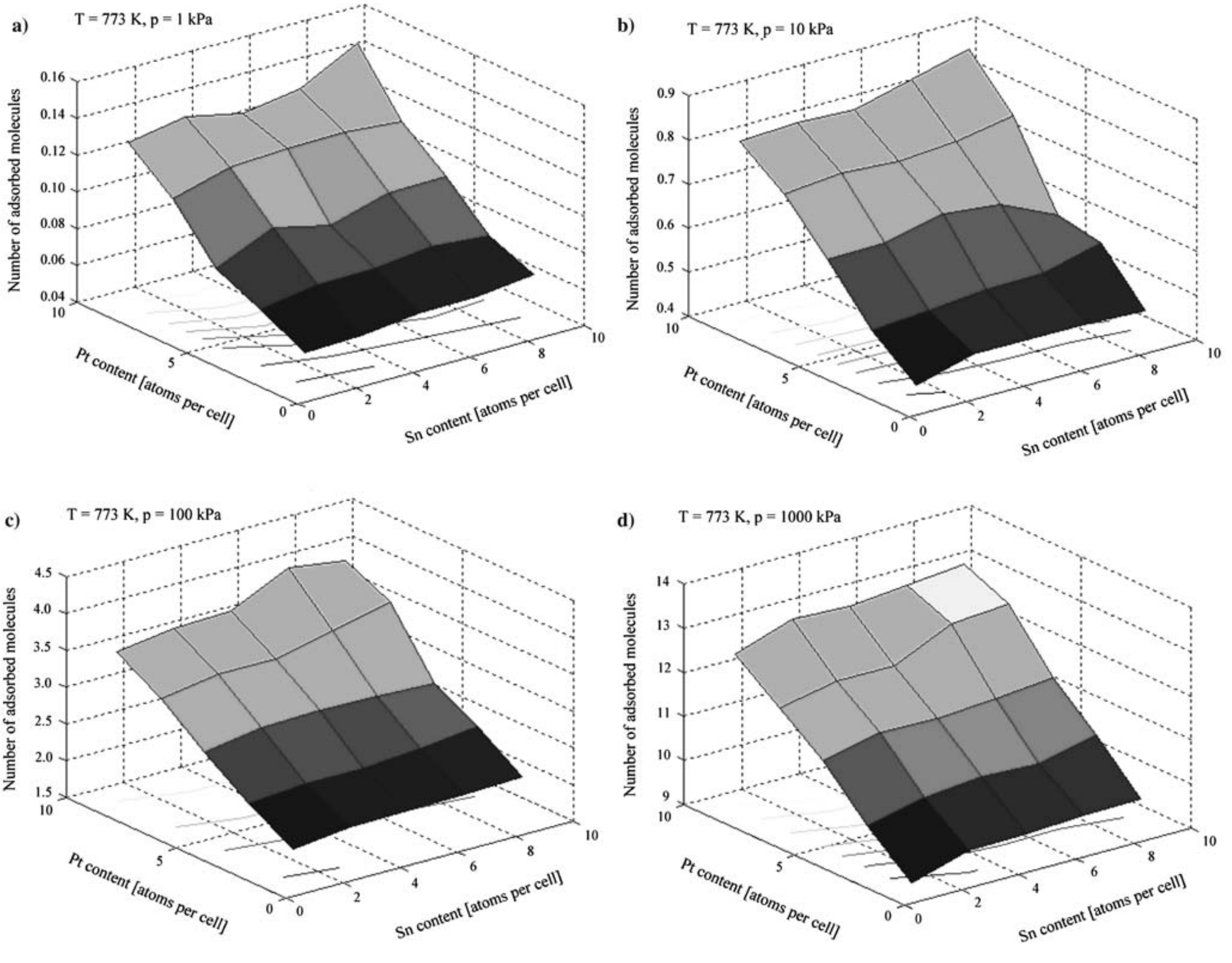

Fig. 11 Number of n-heptane molecules adsorbed at 773 K and 1 kPa (a), 10 kPa (b), 100 kPa (c) and 1000 kPa (d), related to the number of Sn and Pt atoms

Acknowledgement The results published were generated at the following computational centers: Wrocław Centre for Networking and Supercomputing, Interdisciplinary Centre for Mathematical and Computational Modeling in Warsaw, Academic Computer Centre "Cyfronet" in Cracow and Academic Computer Center in Gdańsk TASK.

References

1. Gómez R, Bertin V, López T, Schifter I, Ferrat G (1996) J Mol Catal A: Chem 109:55–66
2. Kluksdahl HE (1968) US Patent 3:415–737
3. Antos GJ, Heights A (1975) US Patent 3:929–683
4. Burch R (1981) J Catal 71:348–359
5. Burch R, Garla LC (1981) J Catal 71:360–372
6. Arteaga GJ, Anderson JA, Rochester CH (1999) J Catal 187:219–229
7. Lieske H, Völter J (1984) J Catal 90:96–105
8. Merlen E, Beccat P, Bertolini JC, Delichère P, Zanier N, Didillon B (1996) J Catal 159:178–188
9. Sexton BA, Hughes AE, Foger K (1984) J Catal 88:466–477
10. Barlett HB (1932) J Am Ceram Soc 15:361–364
11. Woods GB, Panagiotopoulos AZ, Rowlinson JS (1988) Mol Phys 63:49–63
12. Razmus DM, Hall CK (1990) AIChE J 37:769–779
13. Casewit CJ, Colwell KS, Rappe AK (1992) J Am Chem Soc 114:10024–10035
14. Casewit CJ, Colwell KS, Rappe AK (1992) J Am Chem Soc 114:10035–10046
15. Casewit CJ, Colwell KS, Rappe AK (1992) J Am Chem Soc 114:10046–10053
16. Hagler AT, Huler E, Lifson S (1974) J Am Chem Soc 96:5319–5327
17. Hagler AT, Lifson S (1974) J Am Chem Soc 96:5327–5335
18. Lifson S, Hagler AT, Dauber P (1979) J Am Chem Soc 101:5111–5121
19. Hagler AT, Lifson S, Dauber P (1979) J Am Chem Soc 101:5122–5130
20. Hagler AT, Dauber P, Lifson S (1979) J Am Chem Soc 101:5131–5141
21. Kitson DH, Hagler AT (1988) Biochemistry 27:5246–5257
22. Kitson DH, Hagler AT (1988) Biochemistry 27:7176–7180
23. Dauber-Osguthorpe P, Roberts VA, Osguthorpe DJ, Wolff J, Genest M, Hagler AT (1988) Proteins 4:31–47
24. Halicioglu T, Pound GM (1975) Phys Stat Sol (a) 30:619—623